European Journal of Wood and Wood Products (2020) 78:1279–1286
https://doi.org/10.1007/s00107-020-01589-8

ORIGINAL

Resin and volatile content of melamine-impregnated paper assessed by near infrared spectroscopy, a simulation of the industrial process using a laboratory-scale gantry

M. Gonçalves[1,2] · Marta Ribeiro[1,2] · N. T. Paiva[2] · J. M. Ferra[2] · J. Martins[1,3] · F. Magalhães[1] · L. Carvalho[1,3]

Received: 20 December 2019 / Published online: 27 August 2020

Abstract
Melamine-impregnated paper is an important component in the production of high pressure laminates and melamine faced boards. The two most vital quality control parameters assessed during the production of impregnated paper are resin content and volatile content. This work explored the creation of near-infrared (NIR) reflectance models to assess these parameters. A laboratory scale computer-controlled high-precision table gantry was also tested for two reasons: to create an NIR profile of an impregnated paper sample, and to calibrate NIR models by moving the probe using the gantry while taking a spectrum. The NIR profile obtained using the gantry reveals that distinct spots on the surface of the paper have different NIR spectra. The use of the gantry for model creation shows similar or improved performance when compared to taking triplicate spectra of a sample on discrete areas. The time taken for sample analysis also was lower with the use of the gantry because only one spectrum was needed, instead of three. The gantry also enables the creation of models to be used at an industrial scale, allowing an increased range of reference values while not depending on the industrial process. The method can be used to improve reflectance NIR models of samples with heterogeneous or rough surfaces.

1 Introduction

Melamine-impregnated paper is a solution broadly used in the production of high pressure laminates (HPLs) and wood-based panels (Chen et al. 2018; Walia 2019). HPLs are produced by applying high pressure (above 5 MPa) and temperature (above 120 °C) to a set of paper sheets impregnated with thermosetting resins. Usually three layers of paper sheets are applied: a core layer composed of kraft paper sheets impregnated with a phenolic resin, a decorative layer composed of a patterned paper impregnated with melamine–formaldehyde resin, and a protective layer constituted of an overlay paper impregnated with melamine–formaldehyde resin (Hunter 1971; European Standard 2005). The application of melamine-impregnated paper to surfacing wood-based panels, namely in melamine faced boards (MFBs), is also done using temperature and pressure, and this process not only provides a decorative finishing to the surface of the panel but also ensures some surface protection (Ayrilmis 2012; European Standard 2017). The decorative paper can have many sorts of finishing patterns or decorations so that the final product can resemble a variety of surfaces (Roberts and Evans 2005).

Usually, manufacturers of impregnated paper determine two quality control parameters: resin content (RC) and volatile content (VC) (Premark and Holdings 1996; Henriques et al. 2017a). These two values are kept under control so that sheets of paper can be stored in a stacked block without sticking and maintain the resin flow and the necessary cross-linking degree (Roberts 2004; Kandelbauer et al. 2010a; Henriques et al. 2017a).

The process of decorative paper impregnation consists of a series of impregnation and drying steps. The impregnation can be done in three distinct ways: using rollers with an adjustable gap between them, a system of various pairs

Electronic supplementary material The online version of this article (https://doi.org/10.1007/s00107-020-01589-8) contains supplementary material, which is available to authorized users.

✉ L. Carvalho
lhcarvalho@estgv.ipv.pt

[1] Faculdade de Engenharia, LEPABE, Universidade Do Porto, Rua Dr. Roberto Frias s/n, 4200-465 Porto, Portugal

[2] EuroResinas, Indústrias Químicas SA, 7520-195 Sines, Portugal

[3] DEMad, Instituto Politécnico de Viseu, Campus Politécnico de Repeses, 3504-510 Viseu, Portugal

of rollers with controllable gap and speed, or by dipping the paper in the resin and then scrapping off the excess. The drying process is based on blowing hot air over the impregnated paper (Allen and Kemp 1995; Kohlmayr et al. 2014). The sequential steps of paper impregnation are: (1) application of the resin to the decorative paper with the first bath resin formulation, (2) drying in the first air dryer, (3) assess the RC after first impregnation (RC_1), (4) coat the face of the impregnated paper with the second bath resin formulation, (5) second air drying, (6) assess RC after second impregnation (RC_2 or simply RC) and assess VC (Figueiredo et al. 2011).

Normally, the RC and VC are determined off-line using a standard precision balance. The determination of VCs also needs a ventilated oven (Laurence et al. 2006). During production, significant portions of impregnated paper go to waste due to the values, or RC and VC values falling out of specification. In fact, estimates show that the waste of this industry is increasing, mainly because the industry is also growing (Ayrilmis 2012).

A viable on-line solution for the analysis of moisture content is the use of near infrared (NIR) spectroscopy. This technology has been successfully applied to many types of solid and liquid materials, specially due to the dominant water band that can be used for quantitative purposes (Clavaud et al. 2017). A common practice in NIR spectroscopy is to use chemometric techniques (Reich 2005). Among these, principal components analysis (PCA) and partial least squares (PLS) are two of the most used methods for data reduction and model creation (Balabin et al. 2007; Fülöp and Hancsók 2009). Previous scientific publications have already applied NIR spectroscopy to assess properties of impregnated paper. Neimanis et al. (1999) used PCA, PLS, and orthogonal signal correction (OSC) to evaluate the moisture content of an oil impregnated paper. That work showed results for a model that predicts low moisture content of impregnated paper. The model had a relatively high range of analysis (between 1 and 8%) and the authors argued that in such a range the paper is affected by bound water present in cellulosic fibers of paper or free water in the cavities of cells or voids between fibers. Dessipri et al. (2003) have also successfully applied NIR spectroscopy to analyze the remaining useful life of impregnated paper with a melamine–formaldehyde (MF) resin using a diffuse reflectance probe. This ageing phenomenon was associated with the RC and VC of the samples. That technique was also patented (Dessipri et al. 2004) and proven to work in an industrial plant.

A complication that arises when creating NIR models for the prediction of decorative paper properties is that there are a wide range of paper colors and grammages. Each type of paper has specific particularities that make them significantly different from each other, so that their NIR spectra differ (Kandelbauer et al. 2010b). This was also demonstrated by Yang et al. (2014), who showed that a PCA methodology could be used to separate different types of papers into clusters within the PCA scores space.

Nakos and Minopoulou (2008) have also applied NIR spectroscopy to assess the VC of impregnated decorative paper at an industrial level. The results obtained showed that NIR models for the determination of VC can be calibrated and achieved an R^2 of calibration of 93.3%. Henriques et al. (2017b) used interval PLS techniques to create models for the assessment of RC and VC off-line and at a laboratory scale. This approach showed that the technique can be used to select the most relevant wavenumbers for the calibration of the models. The same work also showed that different types of paper in terms of color and grammage also produce distinct NIR spectra.

To further study NIR technology applied to impregnated paper, this work aims to (1) characterize the surface of decorative paper impregnated with an MF resin using NIR spectroscopy and (2) simulate the in-line use of this technology at industrial level using a laboratory scale computer-controlled high-precision table gantry (hereinafter referred to as gantry).

2 Materials and methods

2.1 Sample preparation

Industrial white paper sheets of 80 g/cm^2 were provided by EuroResinas–Indústrias Químicas S.A.. The color chosen for the experiment was based on the volume of production; white paper tends to be produced in larger quantities due to demand. The sheets were then cut in circles with a diameter of 11.3 cm. A total of 100 samples were obtained this way. The samples were later separated in blocks of 10 and put in an oven at 160 °C for different times varying from 0 to 45 s. This procedure was done to artificially create samples with different values of RC and VC.

2.1.1 Sample characterization

The RC is determined by weighing the paper sample prior to and after resin impregnation. Expression 1 shows the equation used to calculate the RC.

$$RC = \frac{m_2 - m_1}{m_1} \tag{1}$$

where m_2 is the mass of paper after impregnation and m_1 is the mass of paper before resin impregnation.

The VCs of impregnated paper are determined by placing the paper sample in a ventilated oven for 5 min. The

expression used to calculate the VC of impregnated paper is presented below:

$$VC = \frac{m_3 - m_4}{m_3} \quad (2)$$

where m_3 is the mass of paper circle before going to a ventilated oven for 5 min at 160 °C, and m_4 is the mass of paper sample after the oven drying step.

2.2 Spectra acquisition

NIR spectra of each paper sample were recorded using a Fourier Transform NIR spectrometer Matrix-F from Bruker with a probe QR400-7-VIS-BX from Ocean Optics. The software used for data acquisition was OPUS 6.5, also from Bruker. The spectra were acquired in reflectance mode but later converted to absorbance. The distance between the end of the reflectance probe and the paper surface (d_p) was optimized using a single impregnated paper sheet and lowering the probe until the peak of the interferogram was maximum, approximately at a distance of 4 mm. This distance was kept throughout all spectral acquisitions.

2.3 Experiment 1: NIR spectra variation along sample surface

The gantry was used for two experiments. Experiment 1 consisted of moving the NIR probe by discrete increments of 200 µm along a line of 8 cm. In each new position of the probe, an NIR spectrum was taken. In total, 40 spectra were acquired. This way, each spectrum was acquired using 8 scans with a resolution of 16 cm^{-1}. The gantry used was a Festo equipment EXCM-30–600-110-KF-ST-B2-E3-EN.

Figure 1 shows the laboratory setup used for the acquisition of data using a gantry.

To help interpret the configuration used, three distances need to be clearly defined: d_g is the distance travelled by the gantry in a straight line (parallel to the table); d_p is the distance between paper surface and the spot where the signal is being captured on the NIR probe (perpendicular to the table); and d_t is the distance between probe and table. The distance between the NIR probe and the table (d_t) was maintained constant. Figure 2 illustrates the explained distances.

2.4 Experiment 2: calibration and validation of RC and VC models

The second experiment consisted of acquiring data for the construction of the RC and VC models. This time the number of scans was 256 and the selected resolution was 16 cm^{-1}, corresponding to 1 min and 40 s of acquisition time.

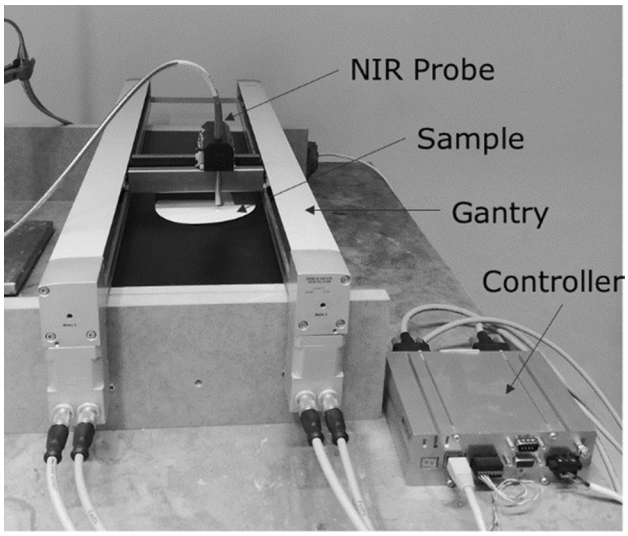

Fig. 1 NIR probe attached to a computer-controlled high-precision table gantry

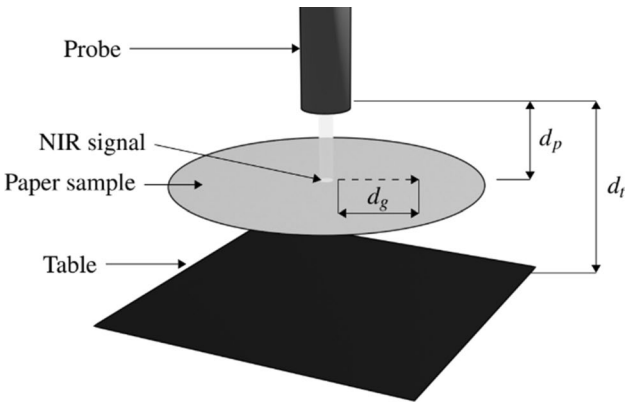

Fig. 2 Scheme of the NIR analysis

The spectra were collected either at discrete spots (method a), or along a continuous path (method b). Method (a) of data acquisition consisted of using the gantry to place the probe on three different spots of the sample and acquiring one spectrum at each location. Method (b) consisted of programing the gantry to move the probe along a specified path over the sample, while continuously obtaining a spectrum. In method (b) only a single spectrum was acquired per sample. The velocity of the probe was optimized so that the probe could cover the maximum surface of the sample during the 256 scans. An illustration of the two acquisition methods is shown in Fig. 3.

Spectra used for the construction of NIR models for the determination of VC and RC were randomly split (70/30) into calibration and validation sets. The NIR models were

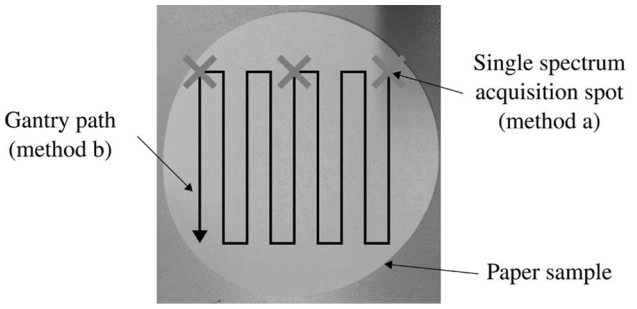

Fig. 3 Illustration of the two types of spectral acquisition. The three crosses represent the locations, where the 3 spectra were taken in method a, the square waved arrow represents the continuous path taken by the gantry in method b

created using Matlab and applying the PLS algorithm distributed in *i*Toolbox (Norgaard et al. 2000).

The models were evaluated using the coefficient of determination (R^2) and the root mean square error (RMSE), calculated using Eq. 3:

$$RMSE_{x,l} = \sqrt{\frac{\sum_{i=1}^{n} \left(\hat{y}_i - y_i\right)^2}{n}} \tag{3}$$

where n is the number of spectra used; i represents each spectrum; $\hat{y}$ is the predicted value using the calibration model; y is the value of the reference method; x can either be substituted by "C" to indicate calibration dataset or "P" to indicate test database; and l can be substituted by:

- N is the data obtained by collecting spectra in discrete locations (method a), the predicted values for each spectrum and paper sample were treated as separated samples (n = 300);
- M is essentially the same as N, but the predicted values for each paper sample were averaged (n = 100);
- G is the data obtained by collecting a spectrum along a continuous path (method b). Only a single spectrum was acquired for each paper sample (n = 100). Please note that method N and M spectra acquisition is three times longer than method G, as there are three spectra being recorded instead of one.

The nomenclature of x and l also applies to the coefficient of determination.

The scheme presented in Fig. 4 easily illustrates the nomenclature used in this work.

The construction of NIR models also involves the study of the best pre-processing technique to use. The pre-processing techniques tested were: inverted signal correction (ISC), first derivative (1deriv), mean-centering (mean), auto-scale (auto), multiplicative signal correction (MSC),

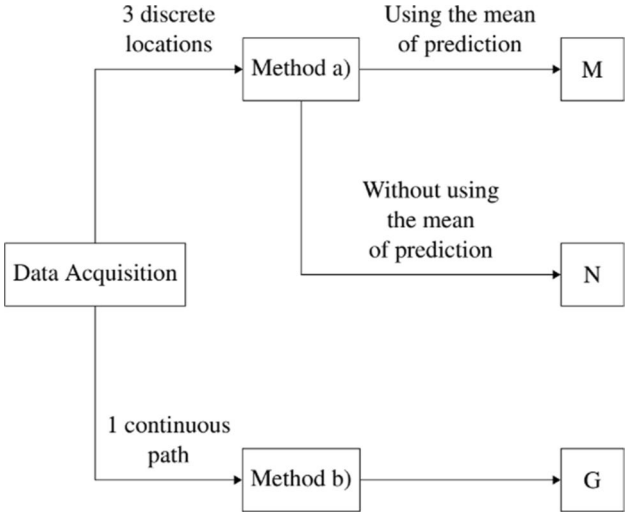

Fig. 4 Schematic of the nomenclature used in this work

standard normal variate (SNV), first derivative + SNV (1deriv + SNV), and second derivative (2deriv).

The goal of using the gantry was to simulate an industrial application of an NIR method at a laboratory scale. In this simulation, the paper specimen stayed fixed and the probe moved in a desired trajectory. However, in an industrial set-up, the paper is usually rolling out of the air driers, this means that one can easily implement this method by fixing the probe above the moving paper.

3 Results and discussion

3.1 Experiment 1: NIR spectra variation along sample surface

The surface of decorative paper presents some roughness at nano, micro, and macro level (Pino et al. 2010), which is in part due to the nature of the paper and in part due to the uneven distribution of resin in the paper during impregnation. To test to which degree this would impact the NIR spectra on the paper surface, the gantry was used to collect the NIR spectra of the surface of the impregnated paper in a straight line with each spectrum separated by 200 µm.

Figure 5 shows the NIR profile obtained by distance travelled (a) and the spectra all layered in the same plot (b) for easier observation of the changes in baseline.

As the gantry travels and distance d_g increases, the baseline of each individual NIR spectrum changes. These changes are explained by differences in the chemical composition of the surface of the paper or the paper roughness. Since the probe remained at a fixed distance from table (d_t), d_p could only increase or decrease due to differences in paper surface height. In other words, if the baseline shifted due

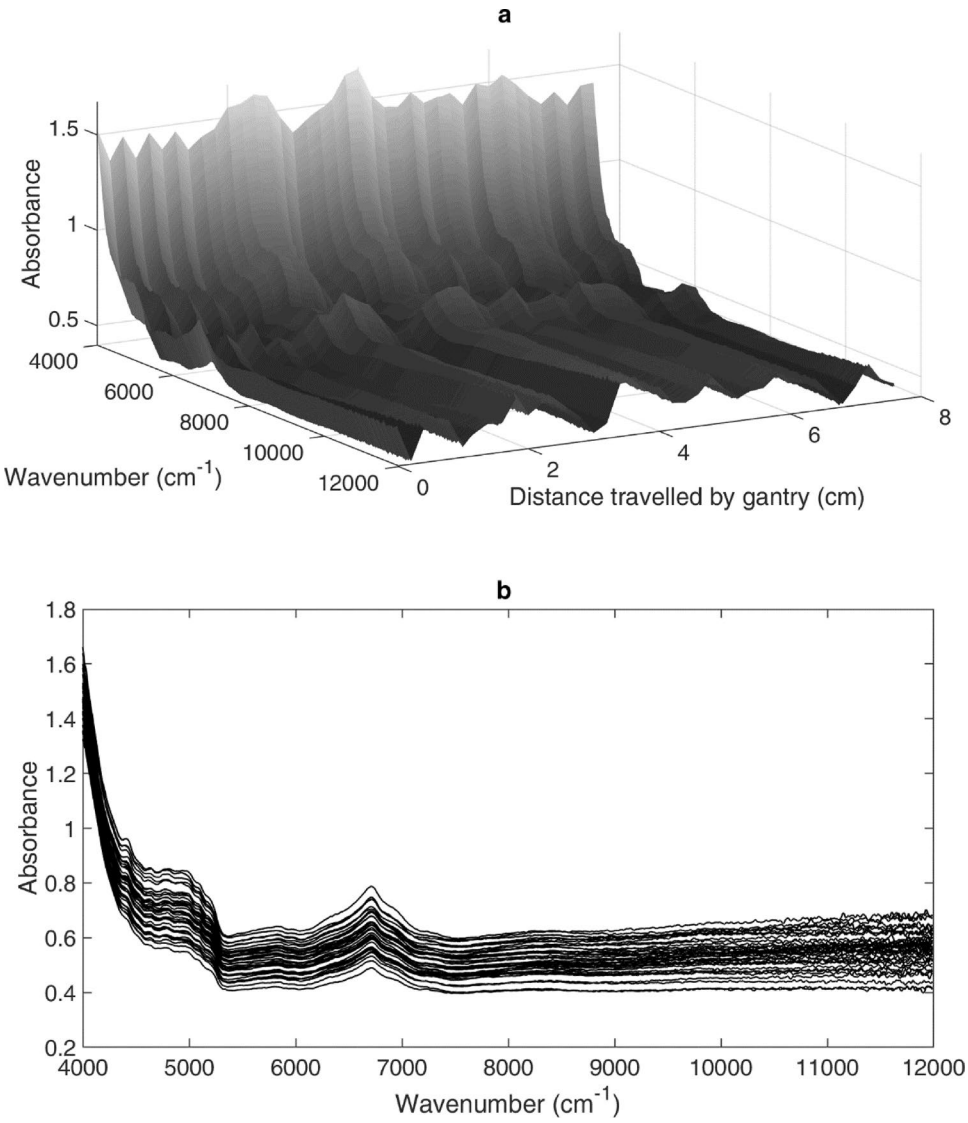

Fig. 5 Straight line profile of NIR spectra of a decorative paper. **a** According to distance travelled by probe, and **b** same spectra without travel distance

to the distance between probe and paper surface, it would be due to the roughness of the paper. Of course, this does not discard the possibility of the chemical properties of the paper also changing.

NIR spectra were collected in reflectance mode, meaning that if the signal arriving at the detector was weaker, the probe was further away from the paper surface and d_p was higher, and vice versa. However, the signal was converted to absorbance, which means that if the baseline of the spectra presented in Fig. 5a, b is lower, more signal is arriving at the detector, meaning that d_p is shorter (the probe is closer to the paper surface); the opposite is also true. The NIR spectra profile obtained presents significant irregularities, which can be due to paper roughness and chemical heterogeneity. This technique could possibly be used to assess the surface profile of the paper sheet using NIR imaging and thus, to evaluate the surface roughness. However, this is outside the scope of this work. The intent of this part of the work is to show that different spots, even relatively close to each other (distances of 200 µm), can have perceivably different NIR spectra.

3.2 Experiment 2: Creation of models to determine resin content and volatile content of impregnated paper

All the results obtained for the creation of NIR models are presented in Tables S1 to S6 (in Electronic Supplementary Material). The best results obtained in terms of RMSEP for each type of data validation for the RC models are presented in Table 1; the same is presented in Table 2 for the case of the VCs. Figure 1S in Supplementary Material shows the predicted values vs. the reference values.

The results show that RMSE values are consistent for both the RC and VC models: method N (without using the means) performed worse than method M (using means), and method G (using the continuous spectra acquisition

Table 1 Best results obtained for the creation of RC models

Validation method	Pre-processing	RMSEC (% m/m)	R_C^2	RMSEP (% m/m)	R_P^2
N	2deriv	0.42	0.41	0.38	0.26
M	Auto	0.40	0.48	0.36	0.31
G	MSC	0.23	0.82	0.29	0.57

Table 2 Best results obtained for the creation of VC models

Validation method	Pre-processing	RMSEC (% m/m)	R_C^2	RMSEP (% m/m)	R_P^2
N	SNV	0.46	0.74	0.32	0.81
M	Mean	0.30	0.90	0.27	0.87
G	1deriv + SNV	0.30	0.90	0.26	0.86

along a path) performed the best. There is only one exception, the calibration results for methods M and G for the VC models, which were equal (0.30% m/m). None of the results obtained for the determination of RC can be considered satisfactory due to the low R^2 (all below 0.6). However, in this case, method G shows some promising results due to performing better than the other methods.

There are two possible reasons for why the RC models performed worse than the VC models. The first is that the NIR has problems in distinguishing the chemical bonds related to resin and to paper. The second is that the distribution of resin could be much more irregular than the distribution of water in the sample. These problems are not so evident in the determination of the VC because this value is mainly attributed to the evaporation of water and formaldehyde from the sample. The use of the gantry partly eliminated the irregularity presented by the sample but was not enough to completely remove this effect. Possibly, the use of NIR imaging could improve these results due to being capable of analyzing a wider surface area and getting a more significant representation of the sample. Unfortunately, this hypothesis could not be tested.

On the other hand, the results obtained for the VC model show some reasonable prediction capability for the M and G method: similar RMSEP (0.27% m/m vs 0.26% m/m) and R_P^2 (0.86 vs 0.87). The better results obtained for methods M and G prove that the samples are irregular, and methods that tend to evaluate the mean over the sample are better suited for these types of material. Even though the M and G methods provided similar results, the time taken for each analysis is different. Since method M needs to take three spectra and method G needs only one spectrum, it can be concluded that method G gets similar or better results with three times less time.

As shown in Tables 1 and 2, the best pre-processing technique to use depends on the method used. Method M got better results when the pre-processing technique of autoscale was used for the RC model and mean-centering alone for the VC model. Method N used second derivative and standard normal variate for the RC and VC. Method G also obtained different results for both RC and VC, MSC and 1deriv + SNV. The differences obtained for the pre-processing of RC and VC can be indicative that the information of RC and VC is different in NIR since the spectra used for RC and VC are the same. This helps in explaining why the VC methods worked best when compared to the RC methods. NIR is a technique that shows reliable results in the analysis of water content of samples when compared to other chemical compounds. Since the determination of VC is influenced by the water present in the papers, one can expect that this method would work better than the RC method.

The creation of NIR methods using at-line approaches results in increased difficulty and time because a continuous process is not easily adjusted to have the necessary range of values. The gantry is a solution that simulates the industrial application of the reflectance probe in an off-line way and at the same time enables the production of samples at a laboratory scale with different reference values. This way the NIR models can be created faster, more reliably, and without needing to stop or alter the production process.

In a practical perspective, the implementation of the methods developed here in a production line would mean a quicker expedition time of the product. However, there are a few considerations that need to be taken into account prior to that. Both VC and RC are determined in the same spot of the production line, so the implementation of one method means the implementation of another, provided that the necessary calibration is done. To be able to fully substitute the traditional methods, NIR methods still need to provide a higher correlation with the more generally accepted methods. This does not necessarily invalidate the implementation of the NIR method for quality control of impregnated paper alongside the weighing methods. The NIR methods can be used to check whether significant changes have occurred in the production of impregnated paper in real-time between two scheduled standard measurements. This would be useful to increase the number of quality-conformant products.

This work also showed that paper roughness has a great impact on NIR methods efficacy. Such roughness can be caused by several process parameters such as resin distribution or temperature profile on the drying step. For an even more refined quality control of the paper, multiple NIR probes could be placed in cross direction on the paper impregnation line so that both directions, cross-section and machine direction, can be covered. The resins used here were of the MF type. Different amino resins such as UF resin could also be used in the production of impregnated

paper (Antunes et al. 2018). For such cases, an NIR methodology may be calibrated and adapted. The paper studied here is of white color. Different paper colors and grammages might need additional NIR methods to be created (Henriques et al. 2017b), as well as papers with different porosities that reflect the amount of resin being incorporated in the paper (Roberts 2004).

4 Conclusion

A melamine impregnated paper sample has a heterogeneous and rough surface, so that spectroscopic methods based on a single localized measurement cannot represent the entirety of the sample. By collecting multiple NIR spectra along the surface of the paper in intervals of 200 µm using a gantry, it was possible to observe the occurrence of spectral baseline shifts. These shifts are due to the heterogeneity and roughness of the paper's surface.

The gantry was also tested to make the NIR probe move while taking a spectrum. This method obtained similar or better results than taking three spectra at different discrete spots of the sample, either by calculating the mean of the prediction values (method M) or without calculating it (method N). The gantry not only improved the results, but also took a third of the analysis time over method M and N and allowed simulating the industrial in-line implementation of the NIR technology to assess the RC and VC. No reliable RC model could be constructed ($R^2 < 0.6$), but the VC model using the gantry showed better results even when only one spectrum was taken per sample ($R_P^2 = 0.86$ and RMSEP = 0.26% m/m). The results obtained here do not seem to indicate that NIR methods should completely substitute more traditional methods, especially if different types of paper are involved. However, the way is paved to use this technology in conjunction with the traditional methods to get a better real-time control of resin impregnation.

Funding This work is a result of the project Operation NORTE-08-5369-FSE-000042 supported by Norte Portugal Regional Operational Programme (NORTE 2020), under the PORTUGAL 2020 Partnership Agreement, through the European Social Fund (ESF). This work was financially supported by project UID/EQU/00511/2019—Laboratory for Process Engineering, Environment, Biotechnology and Energy—LEPABE funded by national funds through FCT/MCTES (PIDDAC). The authors also wish to thank EuroResinas—Indústrias Químicas and project Innosurf (POCI-01-0247-FEDER-33768) under PT2020 for the support with data, equipment and materials.

Compliance with ethical standards

Conflict of interest The author(s) declare no potential conflicts of interest with respect to the research, authorship, and/or publication of this article.

References

Allen P, Kemp MF (1995) Chapter 7—decorative laminates. In: Simpson WG (ed) Plastics: surface and finish (2), 2nd edn. The Royal Society of Chemistry, pp 113–135

Antunes A, Paiva N, Ferra J et al (2018) Highly flexible glycol-urea-formaldehyde resins. Eur Polym J 105:167–176. https://doi.org/10.1016/j.eurpolymj.2018.05.037

Ayrilmis N (2012) Enhancement of dimensional stability and mechanical properties of light MDF by adding melamine resin impregnated paper waste. Int J Adhes Adhes 33:45–49. https://doi.org/10.1016/j.ijadhadh.2011.11.001

Balabin RM, Safieva RZ, Lomakina EI (2007) Comparison of linear and nonlinear calibration models based on near infrared (NIR) spectroscopy data for gasoline properties prediction. Chemom Intell Lab Syst 88:183–188. https://doi.org/10.1016/J.CHEMOLAB.2007.04.006

Chen W, Li S, Feizbakhshan M et al (2018) TiO 2 -SiO 2 nanocomposite aerogel loaded in melamine-impregnated paper for multifunctionalization: formaldehyde degradation and smoke suppression. Constr Build Mater 161:381–388. https://doi.org/10.1016/j.conbuildmat.2017.11.129

Clavaud M, Roggo Y, Dégardin K, Sacre P-Y, Hubert P, Ziemons E (2017) Global regression model for moisture content determination using near-infrared spectroscopy. Eur J Pharm Biopharm 119:343–352. https://doi.org/10.1016/J.EJPB.2017.07.007

Dessipri E, Chryssikos G, Gionis V, Panagiotis N., Alkiviadis P. (2004) Method for assessing remaining useful life and overall quality of laminating paper**.** Patent WO/2002/061404

Dessipri E, Minopoulou E, Chryssikos G et al (2003) Use of FT-NIR spectroscopy for on-line monitoring of formaldehyde-based resin synthesis. Eur Polym J 39:1533–1540. https://doi.org/10.1016/S0014-3057(03)00073-9

European Standard (2005) EN438 High-pressure decorative laminates (HPL)—sheets based on thermosetting resins (usually called laminates)—part 2: determination of properties

European Standard (2017) EN14322 Wood-based panels. Melamine faced board for interior uses. Definition, requirements and classification

Figueiredo AB, Evtuguin DV, Monteiro J, Cardoso EF, Mena PC, Cruz P (2011) Structure-surface property relationships of kraft papers: Implication on impregnation with phenol-formaldehyde resin. Ind Eng Chem Res 50:2883–2890. https://doi.org/10.1021/ie101912h

Fülöp A, Hancsók J (2009) Comparison of calibration models based on near infrared spectroscopy data for the determination of plant oil properties. Hung J Ind Chem 37. 10.1515/238

Henriques A, Gonçalves M, Paiva N, Ferra J, Martins J, Magalhaes FD, Carvalho LH (2017a) Chapter 1—Introduction of advanced functionalities in laminates for wood-based panels: surface quality evaluation. In: Davim JP, Aguilera A (eds) Wood composites materials, manufacturing and engineering [Internet], 1st edn. De Gruyter, Berlin, Boston, pp 1–32. https://www.degruyter.com/view/books/9783110416084/9783110416084-001/9783110416084-001.xml

Henriques A, Gonçalves M, Paiva N, Ferra J, Martins J, Magalhaes FD, Carvalho LH (2017) Determination of resin and moisture content in melamine-formaldehyde paper using near infrared spectroscopy. J Near Infrared Spectrosc 25:311–323

Hunter WM (1971) Chapter 12—decorative laminates. In: Pinner SH, Simpson WGBT (eds) Plastics surface and finish, 1st edn. Butterworth-Heinemann, pp 187–216

Kandelbauer A, Petek P, Medved S, Pizzi A, Teischinger A (2010a) On the performance of a melamine-urea-formaldehyde resin for decorative paper coatings. Eur J Wood Prod 68:63–75. https://doi.org/10.1007/s00107-009-0352-y

Kandelbauer A, Wuzella G, Dolezel-Horwath E, Kessler R (2010b) On-line determination of material properties in laminates manufacture by NIR Spectroscopy. In: Teischinger A, Barbu MC, Dunky M et al (eds) Processing technologies for the forest and biobased products industries PTF BPI. Salzburg, pp 34–35

Kohlmayr M, Stultschnik J, Teischinger A, Kandelbauer A (2014) Drying and curing behaviour of melamine formaldehyde resin impregnated papers. J Appl Polym Sci 131:1–9. https://doi.org/10.1002/app.39860

Laurence KJ, Drees TP, Francis KO, Fairbanks B (2006) Decorative laminate assembly and method of producing same. Patent US7081300B2

Nakos P, Minopoulou E (2008) Novel process control for the resin and panel industries based on FT-NIR. In: 5th European Wood-Based Panel Symposium. Hanover, pp 1–6

Neimanis R, Lennholm H, Eriksson R (1999) Determination of moisture content in impregnated paper using near infrared spectroscopy. In: 1999 Annual Report Conference on Electrical Insulation and Dielectric Phenomena (Cat. No.99CH36319), vol 1, pp 162–165

Norgaard L, Saudland A, Wagner J, Nielsen JP, Munck L, Engelsen SB (2000) Interval partial least-squares regression (iPLS): a comparative chemometric study with an example from near-infrared spectroscopy. Appl Spectrosc 54:413–419

Pino A, Pladellorens J, Colom J (2010) Method of measure of roughness of paper based in the analysis of the texture of speckle pattern. In: AAG Jr., Kaufmann GH (eds) Speckle 2010: optical metrology. SPIE, pp 560–566

Premark RWP Holdings I (1996) Method of impregnating decorative paper with melamine resin EP1225278A2

Reich G (2005) Near-infrared spectroscopy and imaging: basic principles and pharmaceutical applications. Adv Drug Deliv Rev 57:1109–1143. https://doi.org/10.1016/j.addr.2005.01.020

Roberts R, Evans P (2005) Effects of manufacturing variables on surface quality and distribution of melamine formaldehyde resin in paper laminates. Compos Part A Appl Sci Manuf 36:95–104. https://doi.org/10.1016/j.compositesa.2003.05.001

Roberts RJ (2004) Liquid penetration into paper. PhD thesis, Department of Applied Mathematics, Research School of Physical Sciences and Engineering and The Australian National University

Walia K (2019) Description-high pressure laminate market 2018–2025 analysis report. Value Mark Res (report)

Yang Z, Zhang M, Pang X, Lv B (2014) Classifications of decorative paper using differential reflection spectrophotometry coupled with soft independent modeling of class analogy. BioResources 9(2):2521–2528